

Below T_c , however, no similar association is possible, in contrast to the acoustic behavior of liquid helium in the region away from T_λ . In the near vicinity of T_c in nickel, both the attenuation and velocity of sound show features similar to those seen near T_λ in liquid helium.

We are indebted to P. C. Hohenberg for frequent discussions of dynamic scaling ideas. We also wish to acknowledge the experimental assistance of V. G. Chirba.

¹L. P. Kadanoff, to be published.

²P. P. Craig and W. I. Goldburg [J. Appl. Phys. **40**, 964 (1969)] give an excellent review of transport properties near a magnetic transition.

³See, for example, B. Golding, Phys. Rev. Letters **20**, 5 (1968).

⁴C. E. Chase, Phys. Fluids **1**, 193 (1958).

⁵M. Barmatz and I. Rudnick, Phys. Rev. **170**, 224 (1968).

⁶R. J. Pollina and B. Lüthi, Phys. Rev. **177**, 841 (1969).

⁷B. I. Halperin and P. C. Hohenberg, Phys. Rev. **177**, 952 (1969).

⁸K. Kawasaki, Solid State Commun. **6**, 57 (1968), and Progr. Theoret. Phys. (Kyoto) **39**, 285 (1968).

⁹The critical frequency is defined as $\omega_c = \omega_0 |k| \xi^{-1}$, where ξ_0 is the frequency of the critical mode and ξ is the correlation length. For an isotropic ferromagnet ω_0 corresponds to spin waves for $T < T_c$ and spin diffusion for $T > T_c$.

¹⁰There is another dividing line defined by $k\xi = 1$, where k is the sound wave vector and ξ is the correlation length. For our frequency range this boundary occurs $\sim 10^{-5}$ °K from T_c which is beyond our experimental resolution.

¹¹M. F. Collins, V. J. Minkiewicz, R. Nathans, L. Passet and G. Shirane, Phys. Rev. **179**, 417 (1969).

¹²D. G. Howard, B. D. Dunlap, and J. G. Dash, Phys. Rev. Letters **15**, 628 (1965).

¹³G. E. Laramore, thesis, University of Illinois, 1969 (unpublished).

PHOTOEMISSION STUDIES OF THE ELECTRONIC STRUCTURE OF EuO, EuS, EuSe, AND GdS

D. E. Eastman, F. Holtzberg, and S. Methfessel
IBM Watson Research Center, Yorktown Heights, New York 10598
(Received 26 June 1969)

Photoemission measurements on the magnetic semiconductors EuO, EuS, and EuSe show emission from $4f^7$ states which lie in the gap above the top of ~ 2 - to 3 -eV-wide valence bands. These measurements, together with optical data, indicate semiconductor energy gaps of 4.3, 3.1, and 3.1 eV for EuO, EuS, and EuSe (all ± 0.4 eV). Metallic GdS shows a narrow occupied conduction band at the Fermi level, in addition to a filled valence band and $4f^7$ state.

The magnetic and semiconducting NaCl-type compounds EuO, EuS, EuSe, and EuTe and their solid solutions with analogous metallic compounds such as GdS are being widely investigated because of their unique magnetic, optical, and transport properties. Observed phenomena such as the Curie-temperature increase with conductivity,¹ giant magnetoresistance at the ferromagnetic Curie temperature,² and large absorption-edge shift with magnetic order³ have been interpreted in terms of various conflicting models of the electronic structure. The position of the localized magnetic $4f^7$ states with respect to the valence band, the width of the intrinsic semiconductor gap, and the character of the empty states at the bottom of the conduction band have been speculated about in several papers.⁴ We have experimentally determined the occupied energy levels in EuO, EuS, and EuSe using photoemission spectroscopy, which measures absolute electron

energies with respect to the Fermi level E_F .

Photoemission energy distribution curves show narrow stationary energy states at ~ 3 , 1, and 1 eV above the top of the valence bands in EuO, EuS, and EuSe, respectively, which are identified as the localized $4f^7$ states. In metallic GdS, we have found a narrow (~ 1 -eV-wide) occupied conduction band at E_F in addition to the $4f^7$ state and the filled valence band. This conduction band is consistent with a partially filled d band. Our measurements confirm the basic energy-band model suggested by Methfessel⁵ for the semiconducting Eu chalcogenides, in which the $4f^7$ state lies in the energy gap between the valence and conduction bands.

Photoemission from EuO was measured in the range $2.5 \text{ eV} \lesssim h\nu \leq 11.6 \text{ eV}$ using a $\langle 100 \rangle$ surface of a single crystal (with ~ 1 -cm dimensions) which was prepared by cleaving in ultrahigh vacuum ($p \lesssim 1 \times 10^{-10}$ Torr). Polycrystalline films of EuS,

EuSe, and GdS were evaporated onto heated substrates ($T \sim 300^\circ\text{C}$) using an electron-beam gun. Film thicknesses were $\gtrsim 1000 \text{ \AA}$. Pressures were $\approx 1 \times 10^{-8}$ Torr during evaporation (rates $\sim 2\text{-}4 \text{ \AA}/\text{sec}$) and were $\lesssim (1\text{-}5) \times 10^{-10}$ Torr during measurements. Stable and reproducible results were obtained for these conditions. However, an oxygen leak of $\sim 10^{-7}$ Torr for a few minutes was sufficient to distort completely the energy distribution curves. Photoemission techniques have been described elsewhere.⁶ The NaCl-type structures of the films were confirmed by x-ray diffraction measurements.

EuO.—Normalized energy-distribution curves (EDC's) are shown in Fig. 1(a). Emission intensities $N(E)$ are plotted versus the initial-state energy $E_i = V_R - h\nu + \phi_c$ with E_F at the origin. V_R is the applied retarding voltage and ϕ_c is the collector work function. Our Au collector had $\phi_c \approx 5 \text{ eV}$. We observe an emission peak at $E_i \sim -1.8 \text{ eV}$ with a leading edge at $\sim -1 \text{ eV}$. This structure does not shift with photon energy (i.e., constant E_i) and is characteristic of transitions from local states as well as nondirect transitions from band states.⁷

This peak is assigned to emission from the $4f^7$ state, since this assignment explains the data more consistently than the possible alternative assignments of (1) impurity states and (2) nondirect transitions from the valence band. Transitions from impurity states are ruled out because of the large observed quantum efficiency ($\sim 10^{-3}$ electron/photon) of this peak. Furthermore, this peak cannot be associated with the valence band, since the strong transitions from lower energies $-4.2 \text{ eV} \gtrsim E_i \gtrsim -7.2 \text{ eV}$ would then be unexplained. The occurrence of similar emission peaks in EuS and EuSe supports our interpretation. The $4f^7$ state is assumed to be localized.⁸ In this case, the observed edge at $\sim -1 \text{ eV}$ in Fig. 1(a) is interpreted as the minimum binding energy for removing a photoelectron from the $4f^7$ state into a conduction band state above ϕ , leaving a $4f^6$ state behind.⁹ The $\sim 1.3 \text{ eV}$ width of the peak can be explained by the spin-orbit splitting of the excited $4f^6$ configuration into multiplet states (7F_J , $J=0, 1, \dots, 6$) which can occur in the absorption process. This explanation is supported by the fact that the photoemission peak has about the same width as the lowest energy optical absorption peak at $h\nu \sim 2 \text{ eV}$ in EuO, which has been interpreted as being broadened by the same $4f^6$ (7F_J) multiplet.

For $h\nu \gtrsim 6 \text{ eV}$, the emission spectrum of EuO is

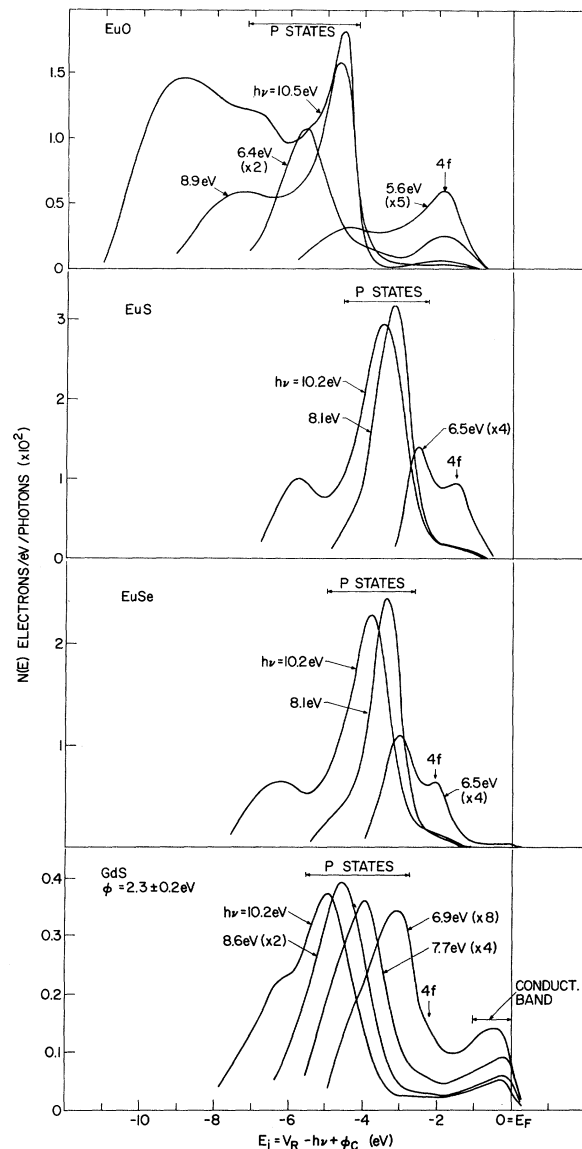


FIG. 1. Photoemission energy-distribution curves for EuO, EuS, EuSe, and GdS. The initial energy is $E_i = V_R - h\nu + \phi_c$, with E_F as origin (V_R is the applied retarding voltage, ϕ_c is the collector work function). The labels (x5), etc., indicate amplification factors.

dominated by transitions from the initial energies $-4.2 \text{ eV} \gtrsim E_i \gtrsim -7.2 \text{ eV}$. These are direct transitions between band states since their initial-state energies change with increasing photon energy.⁷ We identify these energies with the valence band which extends from $\sim -4.2 \text{ eV}$ to $\sim -7.2 \text{ eV}$ below E_F . A schematic representation of the energy levels of EuO is shown in Fig. 2. Band states and local $4f$ states are distinguished by showing them to the right and left of the energy ordinate, respectively. The conduction-band minimum is es-

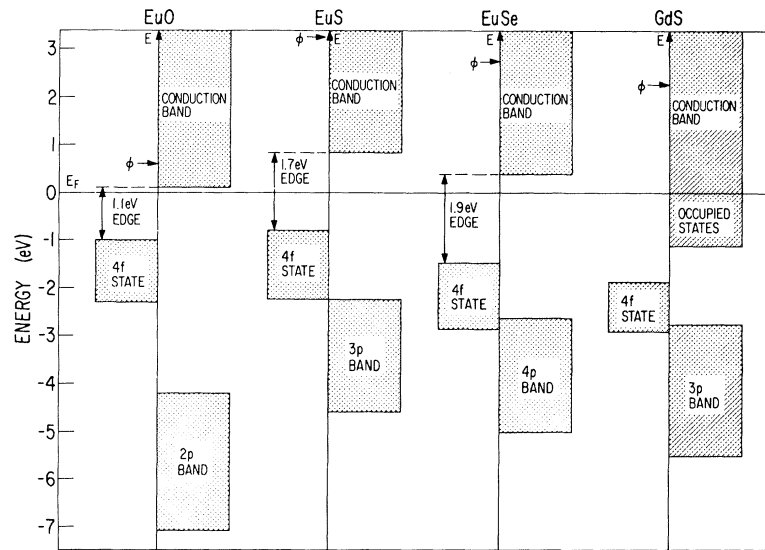


FIG. 2. Schematic representation of energy levels in EuO, EuS, EuSe, and GdS. Energy bands and local $4f^7$ levels are shown to the right and left of the energy ordinate, respectively. The dashed lines represent the lowest excited state of the $4f^7$ level. The $4f^7$ levels are shown with the observed widths. For localized $4f^7$ states, the upper edge represents the minimum binding energy, and the width is due to multiplet broadening (see text).

timated to be ~ 1.1 eV above the top of the $4f^7$ state, i.e., ~ 0.1 eV above E_F . This assignment is based on the observed 1.1-eV optical absorption edge¹⁰ and the occurrence of photoconductivity at this energy.¹¹ An intrinsic semiconductor gap of $\sim 4.3 \pm 0.4$ eV is then obtained for EuO, which corresponds quite well with the second absorption edge.⁹

A very low work function $\phi = 0.6 \pm 0.3$ eV was determined for the $\langle 100 \rangle$ surface of EuO by measuring the retarding voltage which saturates the photocurrent (contact-potential difference between emitter and collector). The measured photothreshold of 2.5 ± 0.2 eV is larger, however, than the value (1.6 ± 0.4 eV) expected from this ϕ . This discrepancy can be due to field distortion at cleavage steps or crystal edges, which can broaden the EDC's at low kinetic energies and lower our value for ϕ .

EuS and EuSe.—Normalized EDC's for EuS [Fig. 1(b)] and EuSe [Fig. 1(c)] show structure similar to that observed for EuO. For EuS and EuSe, respectively, emission is observed from stationary states with peaks at $E_i = -1.5$ and -2 eV and leading edges at ~ -0.8 and ~ -1.4 eV. This structure is again assigned to the $4f^7$ states in EuS and EuSe (see Fig. 2). For $h\nu \geq 6.5$ eV, the emission is dominated by transitions from valence-band states with ~ -2.2 eV $> E_i \gtrsim -4.5$ eV for EuS and ~ -2.6 eV $\gtrsim E_i \gtrsim -5$ eV for EuSe.

The optical absorption edges¹⁰ of 1.7 eV (EuS)

and 1.9 eV (EuSe) for excitation of the $4f^7$ state as well as the observation of photoconductivity^{12,13} at these energies have been used as a basis for placing the conduction-band minima at $+0.8$ eV (EuS) and $+0.5$ eV (EuSe) above E_F . These estimates result in semiconductor gaps of 3.1 ± 0.3 eV for both EuS and EuSe, which are in approximate agreement with the second absorption edges.¹⁰

The work function ϕ of EuS was determined from the contact-potential difference as $\phi = 3.3 \pm 0.3$ eV. The observed photothreshold of ~ 4.0 eV corresponds to excitations from $4f^7$ states at 0.7 eV below E_F . For EuSe, very low-intensity emission (quantum efficiency $< 10^{-4}$) is observed [Fig. 1(c)] from energies $E_F > E_i > -1.4$ eV, which is attributed to impurity-state emission. The measured photothreshold for EuSe of 2.8 ± 0.3 eV is the same as the work function, $\phi = 2.8 \pm 0.3$ eV, due to emission from impurity states at E_F .

GdS.—We studied GdS because it is the metallic counterpart of the Eu chalcogenides, with the same crystal structure and $4f^7$ configuration. In contrast to EuS, etc., the EDC's of GdS [Fig. 1(d)] show strong emission from states within ~ 1 eV of E_F , which we assign to a partially filled conduction band. The narrow (~ 1 eV) width of this band (which presumably contains ~ 1 electron/Gd atom) is consistent with a partially filled d band.¹⁴ Strong emission is observed from initial energies -2.6 eV $\gtrsim E_i \gtrsim -5.5$ eV, which we assign

to an occupied band similar to the valence band of EuS.¹⁵ The top of this band (at $E_f \sim -2.6$ eV) corresponds to the onset of strong interband optical absorption at $h\nu \approx 3$ eV in GdS.¹⁶

Weak stationary structure at $E_f \approx -2.2$ eV in Fig. 1(d) is tentatively assigned to the $4f^7$ state since it is similar (in relative emission strength and width) to the analogous structure assigned to the $4f^7$ states in EuO, EuS, and EuSe. It is interesting that the absorption spectrum¹⁶ of evaporated GdS films does not show an absorption peak corresponding to an excitonlike $4f^7-4f^65d$ transition as seen in the semiconducting Eu chalcogenides.

A work function of $\phi = 2.3 \pm 0.2$ eV was determined for GdS using a Fowler plot. The quantum efficiency of GdS is $\sim \frac{1}{10}$ that of the Eu chalcogenides; this is characteristic of the much shorter mean free path for inelastic electron-electron scattering in a metal.

The energy levels for GdS and EuS in Fig. 2 show an interesting and simple relation. In GdS, the conduction band moves closer to the top of the valence band and becomes partially filled (~ 1 eV wide), while the $4f^7$ level lies just above the valence band for both compounds.

The authors gratefully acknowledge the help of M. W. Shafer who supplied us with the EuO crystal and the able assistance of J. Donelon in performing the measurements.

¹F. Holtzberg, T. R. McGuire, S. Methfessel, and J. C. Suits, *Phys. Rev. Letters* **13**, 18 (1964).

²S. von Molnar and S. Methfessel, *J. Appl. Phys.* **38**, 959 (1967).

³G. Busch, P. Junod, and P. Wachter, *Phys. Letters* **12**, 11 (1964).

⁴For a detailed review see S. Methfessel and D. C. Mattis, in *Encyclopedia of Physics*, edited by S. Flügge (Springer-Verlag, Berlin, Germany, 1968), Vol. 18, Pt. I, pp. 389-562.

⁵S. Methfessel, *Z. Angew. Phys.* **18**, 414 (1965).

⁶D. E. Eastman and W. F. Krolkowski, *Phys. Rev. Letters* **21**, 623 (1968).

⁷C. N. Berglund and W. E. Spicer, *Phys. Rev.* **136**, A1044 (1964).

⁸An alternative explanation of the observed width of the $4f^7$ state is overlap with neighboring ions in the ground state (i.e., a $4f^7$ "band" state); this possibility cannot be eliminated by our measurements but is considered unlikely. A fraction of the observed width can also be due to electron scattering as well as experimental broadening.

⁹All energy levels are measured relative to E_F . The effect of impurities, etc., on E_F in semiconductors, however, will not perturb the separations of observed levels.

¹⁰M. J. Freiser, F. Holtzberg, S. Methfessel, G. D. Pettit, M. W. Shafer, and J. C. Suits, *Helv. Phys. Acta* **41**, 832 (1968).

¹¹T. Penney, private communication.

¹²R. Bachmann and P. Wachter, *Phys. Letters* **26A**, 478 (1968).

¹³S. Methfessel, D. E. Eastman, F. Holtzberg, T. R. McGuire, T. Penney, M. W. Shafer, and S. von Molnar, to be published.

¹⁴A low-density s -like band could lie in the gap below -1 eV for GdS in Fig. 2; such a band would be masked by scattering effects and would be undetectable in the present work.

¹⁵This emission peak is not due to secondary emission since it becomes separated from a secondary emission peak for $h\nu \gtrsim 10$ eV [this separation is observed for $h\nu = 10.2$ eV in Fig. 1(d)].

¹⁶Unpublished data.

PRECISE COMPARISON OF THE JOSEPHSON FREQUENCY-VOLTAGE RELATION AT MICROWAVE AND FAR-INFRARED FREQUENCIES*

T. F. Finnegan, A. Denenstien,[†] D. N. Langenberg, J. C. McMenamin, D. E. Novoseller, and L. Cheng

Department of Physics and Laboratory for Research on the Structure of Matter, University of Pennsylvania, Philadelphia, Pennsylvania 19104

(Received 20 June 1969)

The Josephson frequency-voltage relation has been compared at frequencies of 9.48 and 891 GHz using radiation-induced steps. The results indicate that the relation is frequency independent over this range within an uncertainty of approximately 1.5 ppm.

The utilization of the ac Josephson effect in high-accuracy determinations of the fundamental physical constant^{1,2} e/h and the realization of the importance of this effect for our overall knowledge of the fundamental physical constants³ and

in voltage standard applications⁴ has engendered considerable interest in the question of whether there may be fundamental limitations or corrections to the existing theory of the effect. The central feature of this theory for the foregoing